AWARD NUMBER: W81XWH-14-1-0576

TITLE: Understanding and Targeting Tumor Microenvironment in Prostate Cancer to Inhibit Tumor Progression and Castration Resistance

PRINCIPAL INVESTIGATOR: Lu, Xin

CONTRACTING ORGANIZATION: The University of Texas MD Anderson Cancer Center
Houston, TX 77030

REPORT DATE: October 2015

TYPE OF REPORT: Annual

PREPARED FOR: U.S. Army Medical Research and Materiel Command
Fort Detrick, Maryland 21702-5012

REPORT DOCUMENTATION PAGE

Form Approved
OMB No. 0704-0188

1. REPORT DATE	2. REPORT TYPE	3. DATES COVERED
October 2015	Annual	30 Sep 2014 - 29 Sep 2015

4. TITLE AND SUBTITLE

Understanding and Targeting Tumor Microenvironment in Prostate Cancer to Inhibit Tumor Progression and Castration Resistance

5a. CONTRACT NUMBER

5b. GRANT NUMBER
W81XWH-14-1-0576

5c. PROGRAM ELEMENT NUMBER

6. AUTHOR(S)

Xin Lu

E-Mail: xlu3@mdanderson.org

5d. PROJECT NUMBER

5e. TASK NUMBER

5f. WORK UNIT NUMBER

7. PERFORMING ORGANIZATION NAME(S) AND ADDRESS(ES)

The University of Texas MD Anderson
Cancer Center
3SCR5.4410, 1881 East Road
Houston, TX, 7054

8. PERFORMING ORGANIZATION REPORT NUMBER

9. SPONSORING / MONITORING AGENCY NAME(S) AND ADDRESS(ES)

U.S. Army Medical Research and Materiel Command Fort Detrick, Maryland 21702-5012

10. SPONSOR/MONITOR'S ACRONYM(S)

11. SPONSOR/MONITOR'S REPORT NUMBER(S)

12. DISTRIBUTION / AVAILABILITY STATEMENT

Approved for Public Release; Distribution Unlimited

13. SUPPLEMENTARY NOTES

14. ABSTRACT

The signaling mechanisms between prostate cancer cells and infiltrating immune cells may illuminate novel therapeutic approaches. During the first year of the award period, utilizing a prostate adenocarcinoma model driven by loss of Pten and Smad4, I identified polymorphonuclear myeloid-derived suppressor cells (MDSCs) as the major infiltrating immune cell type which accumulates in the tumor microenvironment and in circulation as the cancer progresses. The MDSCs display potent immunosuppressive activity to limit T cell proliferation. Importantly, depletion of MDSCs with either anti-Gr1 antibody or a MDSC-targeting peptibody blocked tumor progression in mice. Employing a novel dual reporter prostate cancer model, epithelial and stromal transcriptomic profiling identified Cxcl5 as a possible cancer-secreted chemokine to attract Cxcr2-expressing MDSCs. Overall, the research accomplished the proposed and approved Statement of Work for the first year and laid a solid foundation for next two years.

15. SUBJECT TERMS

Prostate cancer, myeloid-derived suppressor cell (MDSC), Pten, Smad4, genetically engineered mouse model, Gr-1, peptide-Fc fusion protein

16. SECURITY CLASSIFICATION OF:			17. LIMITATION OF ABSTRACT	18. NUMBER OF PAGES	19a. NAME OF RESPONSIBLE PERSON
a. REPORT	b. ABSTRACT	c. THIS PAGE			USAMRMC
Unclassified	Unclassified	Unclassified	Unclassified	12	19b. TELEPHONE NUMBER *(include area code)*

Table of Contents

Page

1. INTRODUCTION

The tumor microenvironment (TME) is comprised of a complex mixture of tumor-associated fibroblasts, infiltrating immune cells, endothelial cells and extracellular matrix proteins and signaling molecules such as cytokines[1-3]. Among the infiltrating immune cells, MDSCs represent a phenotypically heterogeneous population of immature myeloid cells that play a tumor-promoting role by maintaining a state of immunological anergy and tolerance[4]. Prostate cancer (PCa) is the most common noncutaneous malignancy in men in the United States. Similar to many other solid tumor types, PCa is characterized by a rich tumor-stroma interaction network that forms the TME[1-3]. MDSCs have been identified recently as a TME constituent in an indolent prostate cancer mouse model with conditional *Pten* deletion[5] and demonstrated to antagonize senescence during early tumorigenesis[6]. However, the molecular mechanisms underlying the recruitment of MDSCs are not well understood and the extent to which MDSCs facilitate PCa progression has not been determined, which the reported research was aimed to explore. Previously, Dr. Ronald DePinho's group showed that deletion of *Pten* in the mouse prostate causes upregulation of Smad4 which constrains cell proliferation and invasion and, accordingly, dual deletion of *Pten* and *Smad4* results in rapid PCa progression including metastasis[7]. In my preliminary data at the time of application to this grant, I performed comparative transcriptomic and cell profile analyses of $Pten^{pc-/-}$ versus $Pten^{pc-/-}Smad4^{pc-/-}$ deficient PCa and revealed a prominent immune signature and resident MDSCs as a major TME population in $Pten^{pc-/-}Smad4^{pc-/-}$ deficient tumors. Through the first year of the award period (Oct 2014 – Sep 2015), I found that there is a stage-dependent increase of infiltrating and circulating granulocytic MDSCs in the mouse model. These MDSCs display potent immunosuppressive activity against T cell proliferation. Consistently, genes involved in ROS production, the major mechanism how granulocytic MDSCs suppress T cells, were found highly upregulated in $Pten^{pc-/-}Smad4^{pc-/-}$ tumors compared with $Pten^{pc-/-}$ tumors. Importantly, immuno-depletion of MDSCs with either Gr-1 antibody or a MDSC-specific peptide-Fc fusion protein[8] dramatically impeded tumor progression in $Pten^{pc-/-}Smad4^{pc-/-}$ mice. The annual progress report described herein using PCa model supports the view that targeting either MDSC recruitment or infiltrated MDSCs may represent a valid therapeutic opportunity in treating advanced prostate cancer. More comprehensive and deeper analysis of MDSCs, as outlined in the Statement of Work (Year 2 -3) should be warranted for mechanism-based molecular target identification and clinical validation for this important immunosuppressive population in PCa.

2. KEYWORDS

Prostate cancer, myeloid-derived suppressor cell (MDSC), Pten, Smad4, genetically engineered mouse model, Gr-1, peptide-Fc fusion protein

3. ACCOMPLISHMENTS

- **What were the major goals of the project?**

The overall goal of the 3-year project was to provide the phenotypic and molecular understanding of MDSCs during the prostate cancer progression in the $Pten^{pc-/-}Smad4^{pc-/-}$ spontaneous metastatic PCa mouse model, and develop biomarkers and/or targetable molecules for MDSCs with functional and clinical validation for bench-to-bedside translation of the research. For the first year that is directly relevant to this annual report, the specific goals included:

1) Characterize MDSCs in the mouse model by identifying the infiltration frequency at different tumor development stages and assessing gene expression and immunosuppressive activity.

2) Determine the functional significance of MDSCs by investigating the phenotyical consequence of depleting MDSCs in tumor progression in the mouse model.

- **What was accomplished under these goals?**

First, more data were collected to corroborate the finding on the prominent infiltration of immune cells in the $Pten^{pc-/-}Smad4^{pc-/-}$ tumor model. Ingenuity Pathway Analysis (IPA) analysis revealed a prominent immune signature including Granulocytes Adhesion and Diapedesis, Leukocytes Extravasation Signaling, and Agrandulocytes Adhesion and Diapedesis as 3 of the top 4 most activated pathways in $Pten^{pc-/-}Smad4^{pc-/-}$ adenocarcinoma compared to tumors in $Pten^{pc-/-}$ mice which are more indolent with high-grade PIN as the main lesion (Figure 1A; p value < 2.03E-7). Correspondingly, immunohistochemical staining (IHC) highlighted

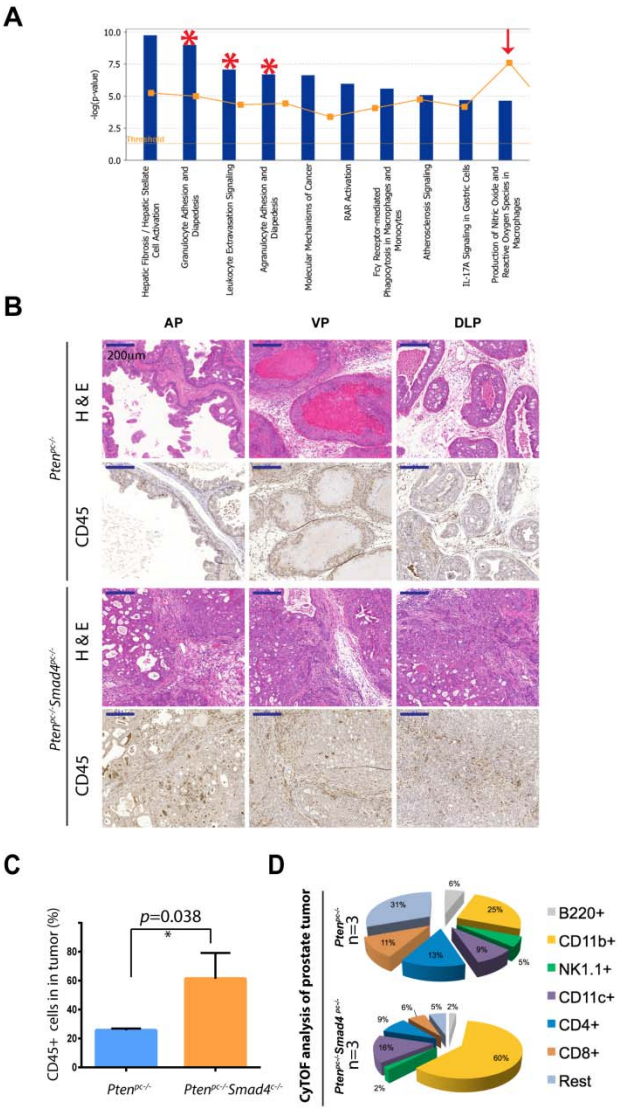

Figure 1. Prominent Infiltration of Immune Cells in the *Pten*$^{pc-/-}$*Smad4*$^{pc-/-}$ Tumors as Compared to *Pten*$^{pc-/-}$ Tumors. **(A)** The top 10 activated pathways in *Pten*$^{pc-/-}$*Smad4*$^{pc-/-}$ tumors (n=5) as compared to *Pten*$^{pc-/-}$ tumors (n=5) identified by Ingenuity pathway analysis (IPA). **(B)** A significant increase in the infiltration of immune cells as shown by IHC for CD45 in *Pten*$^{pc-/-}$*Smad4*$^{pc-/-}$ tumors as compared to *Pten*$^{pc-/-}$ tumors from 16 weeks old mice (n=3). AP, VP and DLP stand for anterior prostate, ventral prostate and dorsolateral prostate, respectively. Scale bar 200 μm. **(C)** Quantification of tumor-infiltrating CD45$^+$ cells (AP, VP and DLP combined) in *Pten*$^{pc-/-}$ tumors and *Pten*$^{pc-/-}$*Smad4*$^{pc-/-}$ from 16 weeks old mice (n=3), assessed by CyTOF. **(D)** Percentages of various immune cell populations within the CD45$^+$ infiltrating immune cells in prostate tumors from 16 weeks old *Pten*$^{pc-/-}$ and *Pten*$^{pc-/-}$*Smad4*$^{pc-/-}$ mice, assessed with CyTOF and analyzed with Flowjo. CD11b+ myeloid cells are significantly more in *Pten*$^{pc-/-}$*Smad4*$^{pc-/-}$ tumor as compared to *Pten*$^{pc-/-}$ tumor (n=3, $P<0.05$).

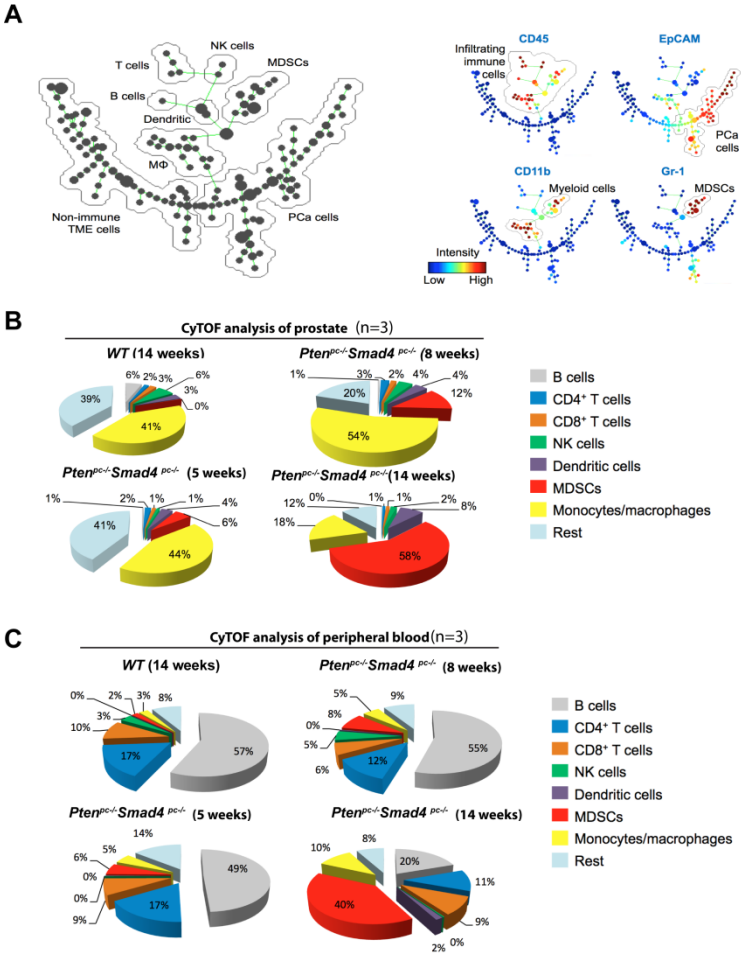

Figure 2. CD11b$^+$ Gr-1$^+$ Cells are Significantly Increased in *Pten*$^{pc-/-}$*Smad4*$^{pc-/-}$ Tumors as Compared to *Pten*$^{pc-/-}$ Tumors. (A) SPADE tree derived from CyTOF (17-marker) analysis of whole tumor cell population from *Pten*$^{pc-/-}$*Smad4*$^{pc-/-}$ mice at 5-week, 8-week, and 14-week old (n=3). Live single cells were used to construct the tree. Cell populations were identified as PCa cells (EpCAM$^+$ CD45$^-$), non-immune TME cells (EpCAM$^-$ CD45$^-$), T cells (CD45$^+$ CD3$^+$ TCRβ$^+$), B cells (CD45$^+$ B220+ CD19+), NK cells (CD45$^+$ NK1.1$^+$), dendritic cells (CD45$^+$ CD11c$^+$), putative MDSCs (CD45$^+$ CD11b$^+$ Gr-1$^+$), and macrophages (CD45$^+$ CD11b$^+$ Gr-1$^-$). On the right panels, the tree is colored by the median intensity of individual markers shown on the top to highlight infiltrating immune cells (EpCAM$^-$ CD45$^+$), epithelial PCa cells (EpCAM$^+$ CD45$^-$), total myeloid cells (CD45$^+$ CD11b$^+$), and putative MDSCs (CD45$^+$ CD11b$^+$ Gr-1$^+$). **(B-C)** CyTOF analysis of tumors (B) or peripheral blood (C) from 5, 8, and 14 weeks old *Pten*$^{pc-/-}$*Smad4*$^{pc-/-}$ mice revealed an age-dependent increase in the MDSCs infiltration. Prostate from wild type (WT) mice at 16-week old was used as control (n=3 for each genotype).

conspicuous infiltration of CD45$^+$ leukocytes in *Pten*$^{pc-/-}$*Smad4*$^{pc-/-}$ tumors (Figure 1B). To comprehensively audit the spectrum of infiltrating immune cells in tumors, I performed mass cytometry (CyTOF) immunophenotyping[9] to catalog tumor cell type constituents from well-established tumors in 16-week old *Pten*$^{pc-/-}$ and *Pten*$^{pc-/-}$*Smad4*$^{pc-/-}$ mice. Employing a 9-marker antibody panel, CyTOF confirmed a significant increase of CD45$^+$ infiltrating leukocytes in *Pten*$^{pc-/-}$*Smad4*$^{pc-/-}$ as compared to *Pten*$^{pc-/-}$ tumors (Figure 1C). Within the CD45$^+$ infiltrating cells, CD11b$^+$ myeloid cells represented a significantly increased immune population in *Pten*$^{pc-/-}$*Smad4*$^{pc-/-}$ as compared to *Pten*$^{pc-/-}$ tumors (Figure 1D).

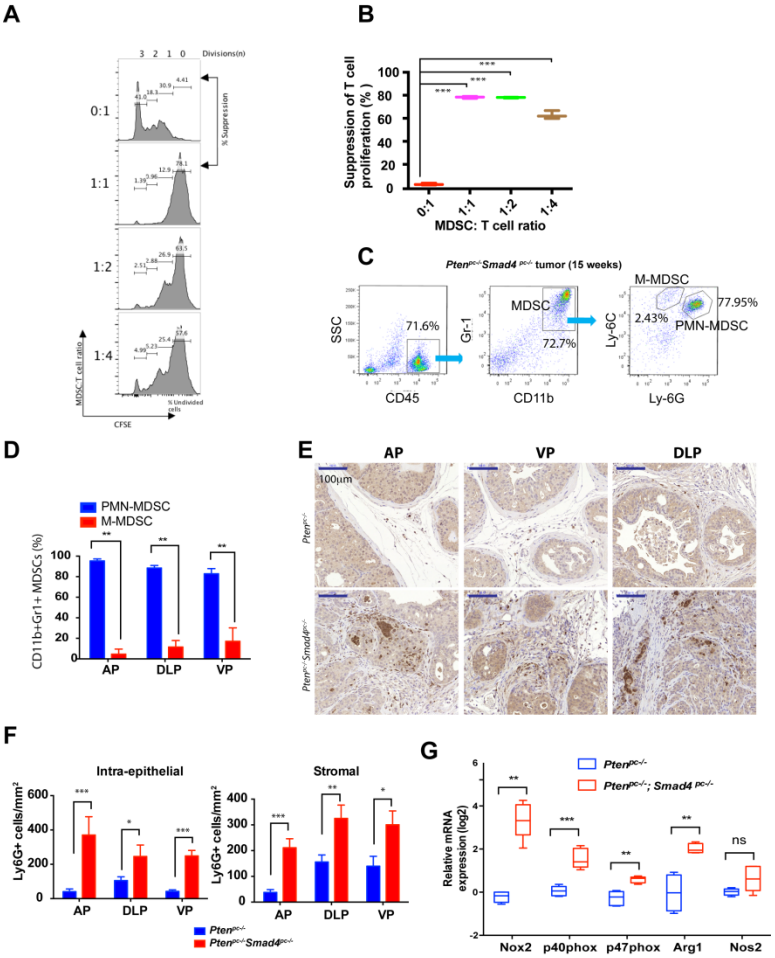

Figure 3. MDSCs from *Pten*$^{pc-/-}$*Smad4*$^{pc-/-}$ Tumors Display Potent Immunosuppressive Activities and are dominated by PMN-MDSCs. (A) CD11b$^+$ Gr-1$^+$ cells from *Pten*$^{pc-/-}$*Smad4*$^{pc-/-}$ tumors display potent immune-suppressive activity towards T cell activation as demonstrated by CFSE dilution assay in triplicate. **(B)** Summarized result from (A). **(C-D)** Flow cytometry analysis shows PMN-MDSCs as the major population in the infiltrated MDSCs in established *Pten*$^{pc-/-}$*Smad4*$^{pc-/-}$ tumors at AP, DLP and VP (n=5). **(E-F)** A significant increase in Ly-6G$^+$ cells in *Pten*$^{pc-/-}$*Smad4*$^{pc-/-}$ tumors as compared to the *Pten*$^{pc-/-}$ tumors as shown by IHC for Ly-6G and quantified by location of positively stained cells in the intra-epithelial or stromal compartment of the tumor at AP, DLP and VP (n=3). **(G)** Quantification of the mRNA expression of subunits of NADPH oxidase (*Nox2*, *p40phox*, and *p47phox*), *Arg1* and *Nos2* in the *Pten*$^{pc-/-}$*Smad4*$^{pc-/-}$ tumors and the *Pten*$^{pc-/-}$ tumors (n=5). In B, D, F and G, **P<0.05, **P<0.01, ***P<0.001.*

To achieve the objective of measuring infiltration frequency of MDSCs and other immune subsets at different tumor stages using CyTOF (**SOW Task 1.1**), serial CyTOF analyses using an expanded antibody panel of 17 surface markers were performed on single cells from primary tumors, peripheral blood, spleen and draining lymph nodes at 5, 8, and 14 weeks of age. The detailed immunophenotyping profiles enabled construction of the SPADE derived tree[9]. SPADE (spanning-tree progression analysis of density-normalized events) is a computational approach to facilitate the identification and analysis of heterogeneous cell types. SPADE of the *Pten*$^{pc-/-}$*Smad4*$^{pc-/-}$ model displays the complexity of the TME which is composed of epithelial tumor cells (EpCAM$^+$ CD45$^-$), non-immune TME cells (EpCAM$^-$ CD45$^-$), and infiltrating immune cells (EpCAM$^-$ CD45$^+$) that can be further grouped into various immune cell subpopulations (Figure 2A). Among the infiltrating immune cells, there was a striking age-dependent increase of CD11b$^+$ Gr-1$^+$ cells in tumors (Figure 2B) and peripheral blood from *Pten*$^{pc-/-}$*Smad4*$^{pc-/-}$ mice (Figure 2C); this trend was much less pronounced in the spleen or draining lymph nodes (data not shown).

CD11b and Gr-1 double positivity only provides a phenotypical marking of these cells as being possible MDSCs. The definition of MDSC requires these cells being immunosuppressive in a standard T cell proliferation assay. Therefore, to assess immunosuppressive activity of the intratumoral CD11b$^+$ Gr-1$^+$ cells (**SOW Task 1.3**), I examined T cell proliferation using a standard cell co-culture system, in which I found that these CD11b$^+$ Gr-1$^+$ cells strongly suppressed CD3 and CD28 antibody-induced T cell proliferation and activation (Figure 3A-B), establishing that CD11b$^+$ Gr-1$^+$ cells are indeed functional MDSCs. MDSCs can be further classified as Ly-6G$^+$ Ly-6C^{Low} subset with polymorphonuclear phenotype (PMN-MDSCs) and Ly-6G$^-$ Ly-6C^{high} subset with monocytic phenotype (M-MDSCs)[10]. PMN-MDSCs represented the major MDSC population in *Pten*$^{pc-/-}$*Smad4*$^{pc-/-}$ tumors (Figure 3C-D), consistent with previously observed preferential expansion of PMN-MDSCs in tumor-bearing mice of various syngeneic models[4,5,10]. The abundance of PMN-MDSCs was further

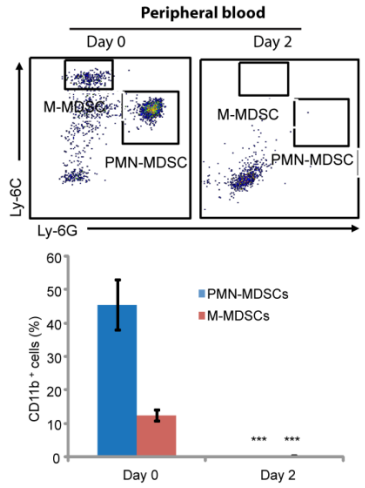

Figure 4. Gr-1 antibody significantly reduced MDSCs in peripheral blood 2 days after 1 dose of injection, measured by Ly-6G and Ly-6C using flow cytometry (n=3).

confirmed by IHC for Ly-6G, as shown by quantification of both intra-epithelial and stromal Ly-6G$^+$ cells in tumors from *Pten*$^{pc-/-}$*Smad4*$^{pc-/-}$ mice and *Pten*$^{pc-/-}$ mice (Figure 3E-F). It has been shown previously that ROS production by PMN-MDSCs is one of the mechanisms driving immune suppression[4,11-13]. Correspondingly, IPA revealed that pathways involved in ROS and NO production are among the top pathways activated in *Pten*$^{pc-/-}$*Smad4*$^{pc-/-}$ tumors (Figure 1A, arrow). Consistent with the increased infiltration of PMN-MDSCs in the *Pten*$^{pc-/-}$*Smad4*$^{pc-/-}$ tumors, the expression of several subunits of NADPH oxidase (Nox2, p40^{phox}, and p47^{phox}), which are responsible for ROS production in PMN-MDSCs [4], were significantly upregulated in *Pten*$^{pc-/-}$*Smad4*$^{pc-/-}$ tumors relative to *Pten*$^{pc-/-}$ tumors (Figure 3G). Moreover, *Arg1*, but not *Nos2*, was highly upregulated in the *Pten*$^{pc-/-}$*Smad4*$^{pc-/-}$ tumors (Figure 3G). These RNA level data addressed the biological parameters of MDSCs in the mouse model (**SOW Task 1.2**), a corroborating finding on their immunosuppressive activity which supports these MDSCs as being *bona fide* MDSCs in the mouse model.

Enrichment of MDSCs in advanced *Pten*$^{pc-/-}$*Smad4*$^{pc-/-}$ tumors prompted us to explore the possible role of MDSCs in tumor progression (**SOW Task 2.1**). Using a well-characterized anti-Gr-1 neutralizing monoclonal antibody (clone RB6-8C5)[14], MDSCs were depleted in *Pten*$^{pc-/-}$*Smad4*$^{pc-/-}$ mice at 14 weeks of age, a point coincident with progression to the early invasive carcinoma stage. The potent MDSC depletion activity of anti-Gr-1 monoclonal antibody was evidenced by significantly decreased PMN-MDSCs and M-MDSCs in peripheral blood as early as day 2 post-treatment (Figure 4). Additionally, a systemic reduction of MDSCs in spleen, bone marrow, and prostate tumors was documented following a 30-day treatment regimen of anti-Gr-1 monoclonal antibody (Figure 5A). This MDSC depletion was accompanied by an increase of CD8$^+$ T cells (so-called killer T cells) (Figure 5A), consistent with elimination of the T cell suppression activity of MDSCs. Importantly, in line with the CD8$^+$ T cell expansion, I observed that the Gr-1 treated prostate displayed remarkable weight reduction in ventral and dorsolateral prostate (VP & DLP) (Figure 5B). The lack of difference in the weight of anterior prostate (AP) is likely due to the fact that AP tend to developed cysts with fluid accumulated inside the gland[15,16], which also prevent the accurate measure of the prostate weight.

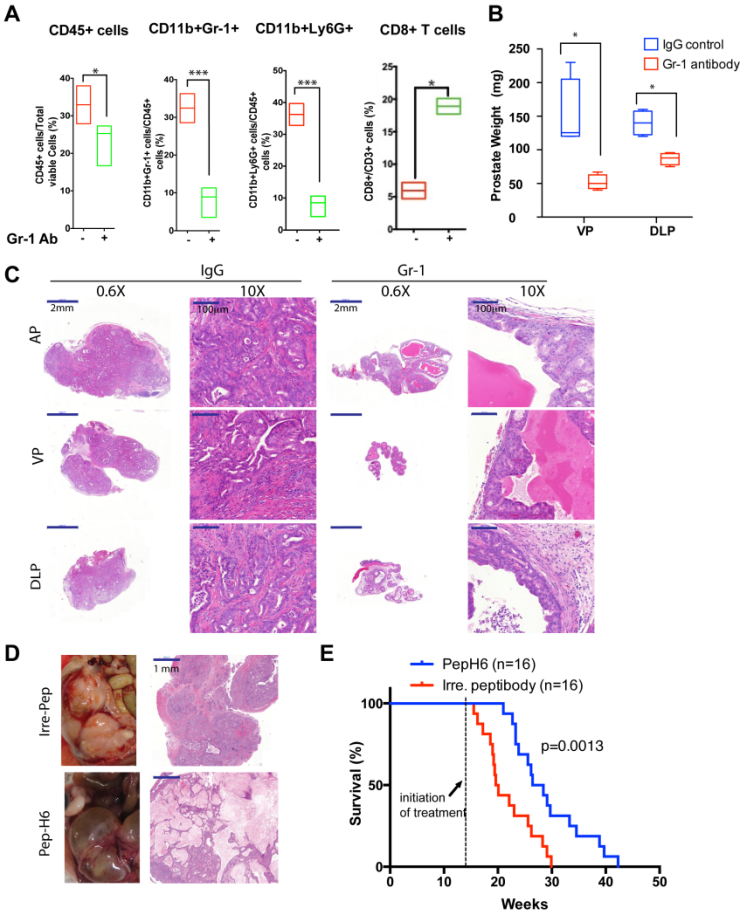

Figure 5. Targeting MDSCs with anti-Gr-1 Neutralizing Antibody or MDSC-specific Peptibody Significantly Delayed Tumor Progression in *Pten*$^{pc-/-}$*Smad4*$^{pc-/-}$ Mice. (A) Administration of Gr-1 neutralizing antibody *in vivo* significantly reduced CD45$^+$ infiltrating immune cells, reduced MDSCs and increased CD8$^+$ T cells among total T cells in *Pten*$^{pc-/-}$*Smad4*$^{pc-/-}$ tumors (n=4), measured by flow cytometry. **(B)** Gr-1 antibody treatment of 14-week old mice significantly reduced the weight of VP and DLP in *Pten*$^{pc-/-}$*Smad4*$^{pc-/-}$ mice. **(C)** Gr-1 antibody remarkably altered the tumor histopathology in *Pten*$^{pc-/-}$*Smad4*$^{pc-/-}$ adenocarcinoma, analyzed by H&E staining of AP, VP and DLP. **(D)** One month of Pep-H6 peptibody treatment led to significant appearance and histology changes of the *Pten*$^{pc-/-}$*Smad4*$^{pc-/-}$ adenocarcinoma. **(E)** Kaplan-Meier survival curve showing the significant delay of mortality caused by Pep-H6 peptibody treatment of *Pten*$^{pc-/-}$*Smad4*$^{pc-/-}$ mice. In A and B, **P<0.05, ***P<0.001.*

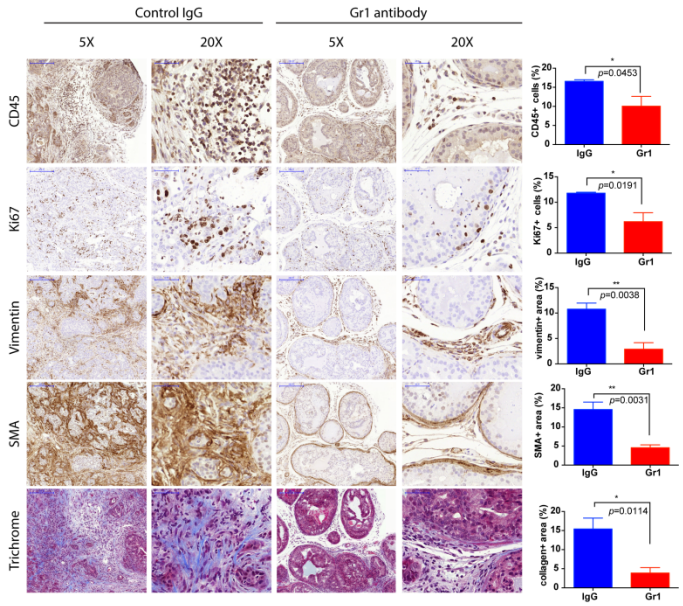

Figure 6. Biology impact of MDSC depletion. IHC staining of Ki67, CD45, Vimentin, Smooth muscle actin (SMA) and Trichrome staining of mouse prostate tissues treated with IgG control or Gr1 antibody. Quantification was performed using ImageJ.

Histopathological analysis revealed adenocarcinoma was the predominant pathology in mice treated with the control IgG whereas mPIN was the predominant morphological presentation in prostates from mice treated with anti-Gr-1 monoclonal antibody (Figure 5C). In addition, by immunohistochemical staining for CD45, Ki67, vimentin, smooth muscle actin (SMA), and Trichrome staining, we observed that tumor remnants in mice treated with anti-Gr-1 monoclonal antibody displayed markedly reduced levels of cellular proliferation, stromal reaction, and inflammation as compared to those tumors treated with control IgG antibody (Figure 6).

I proposed to use CD11b-DTR inducible allele to deplete MDSCs in the $Pten^{pc-/-}Smad4^{pc-/-}$ mice, which should provide a genetic method for MDSC functional evaluation. Currently, the compound mouse $Pten^{pc-/-}$ $Smad4^{pc-/-}$ $CD11b\text{-}DTR^{+}$ are still in the process of generation through multi-generational cross, therefore, this stated goal (**SOW Task 2.2**) is not met yet. Nevertheless, aimed to eventually develop MDSC depletion as a potential therapeutic approach to PCa treatment, I took an alternative approach and utilized the recently developed MDSC-specific peptide-Fc fusion protein (i.e., peptibodies) at MD Anderson Cancer Center that has been shown to effectively eliminate MDSCs *in vivo* through targeting the S100A9 surface protein[8]. Employing a hydrodynamic injection approach for nucleic acid delivery[17], intravenous injection of either Pep-H6 peptibody expression vector or irrelevant control peptibody vector were initiated at 14 weeks every 4 days in $Pten^{pc-/-}Smad4^{pc-/-}$ mice. Strikingly, a single injection of the Pep-H6 peptibody significantly reduced the MDSCs in the peripheral blood, whereas such effect was not observed using the irrelevant control peptibody (Figure 7). Pep-H6 peptibody treatment for one month led to a dramatic decrease in cancer cell content in the prostate tumors (Figure 5D) and provided significant survival benefit for tumor-bearing mice (Figure 5E). Due to the specificity of Pep-H6 in depleting MDSCs but not other myeloid cells[8], this result may have the merit to substitute for the CD11b-DTR approach which actually targets all myeloid cells that express CD11b. Together, my data strongly support the view that MDSC depletion blocks prostate tumor progression in the $Pten^{pc-/-}Smad4^{pc-/-}$ model, fulfilling the major objective of first year research as outlined in approved SOW.

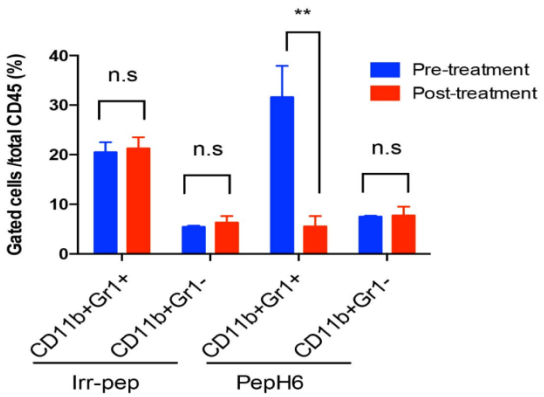

Figure 7. Pep-H6 peptibody treatment significantly reduced MDSCs in peripheral blood 3 days after 1 dose of injection measured by flow cytometry(n=3). *$P<0.05$, **$P<0.01$.

Another subtask was to test the sufficiency of MDSCs isolated from $Pten^{pc-/-}Smad4^{pc-/-}$ mouse to support growth of prostate cancer cells isolated from the $Pten^{pc-/-}$ tumors which are of feeble growth potential and invasiveness[18] through a tumor-MDSC recombination assay in syngenetic C57BL/6 mice (**SOW Task 2.3**). While both $Pten^{pc-/-}Smad4^{pc-/-}$ and $Pten^{pc-/-}$ have been backcrossed to C57BL/6 background thus syngeneic transplantation was enabled, the key experimental design of this recombination assay was to equip $Pten^{pc-/-}$ with both mTmG allele (to allow sorting GFP^{+} cancer cells) and LSL-luciferase allele (to allow bioluminescence imaging to track both primary tumor growth and possibly metastasis) before isolating cancer cells and recombining with MDSCs isolated from reporter-free $Pten^{pc-/-}Smad4^{pc-/-}$ mice. Currently, the former mouse, $PB\text{-}Cre^{+}$ $Pten^{L/L}$ $mTmG^{L/+}$ $LSL\text{-}Luc^{L/+}$, are being developed to the last stage and the first recombination assay is expected to take place in 1-2 months.

Finally, excited by the depletion experiment result, I have started searching for molecular mechanism

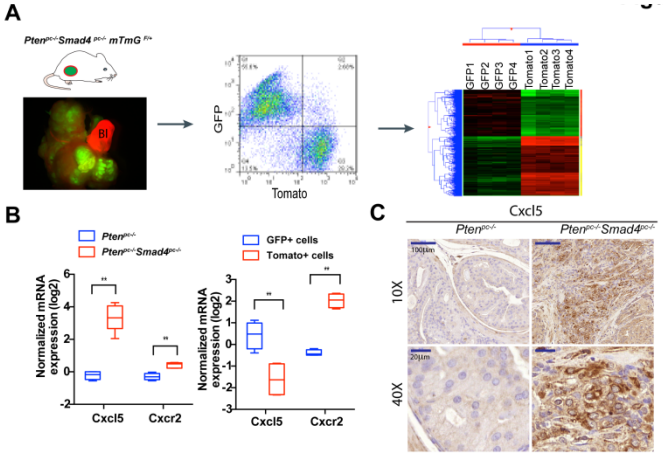

Figure 8. Cxcl5-Cxcr2 axis may be relevant to the recruitment of MDSC. (A) Establishment of *Pten*$^{pc-/-}$*Smad4*$^{pc-/-}$*mTmG*$^{+}$ model allows fluorescent visualization of the GFP^{+} tumor cells intermixed with Tomato^{+} stroma (Left Panel); FACS isolation of GFP^{+} tumor cells and Tomato^{+} stromal cells from the prostate adenocarcinoma (Middle Panel); microarray analysis to identify differentially expressed genes (Right Panel). In the fluorescence image, Bl denotes bladder (completely Tomato^{+}) (n=2). **(B)** Quantification of mRNA expression shows that *Cxcl5* and *Cxcr2* were both expressed at higher levels in *Pten*$^{pc-/-}$*Smad4*$^{pc-/-}$ tumors than *Pten*$^{pc-/-}$ tumors, and *Cxcl5* expression was enriched in GFP^{+} tumor cells, whereas *Cxcr2* in Tomato^{+} stromal cells. (n=5) **(C)** IHC for Cxcl5 showed significantly higher expression levels of *Cxcl5* in *Pten*$^{pc-/-}$*Smad4*$^{pc-/-}$ tumors than *Pten*$^{pc-/-}$ tumors (n=3).

that may account for the accumulation of MDSCs in the *Pten*$^{pc-/-}$*Smad4*$^{pc-/-}$ tumors. At the time of applying for this grant, I had incorporated *mTmG* dual fluorescence reporter allele into the *Pten*$^{pc-/-}$*Smad4*$^{pc-/-}$ model where signaling events between tumor cells and stroma can be precisely delineated. The *mTmG* allele[19] allows Cre-dependent GFP expression in prostate epithelial cells and ubiquitous tdTomato expression in all other non-Cre expressing cells (Figure 8A). Transcriptomic and IPA analyses of FACS-sorted GFP^{+} tumor cells and Tomato^{+} stromal cells showed distinct expression patterns by hierarchical clustering (Figure 8A) with tumor cells enriched for pathways involved in cell adhesion molecules and tight junction (consistent with their epithelial nature) and stromal cells displaying activation of more diverse pathways involved in chronic inflammation, such as cytokine/cytokine receptor interaction, and chemokine, Jak-STAT, TCR, and BCR signaling ($p<0.01$, data not shown). This result is consistent with the immuno- and histopathological analyses showing a massive infiltration of immune cells in the *Pten*$^{pc-/-}$*Smad4*$^{pc-/-}$ tumors. Employing this new model, I sought to identify genes that were upregulated in *Pten*$^{pc-/-}$*Smad4*$^{pc-/-}$ cancer cells relative to *Pten*$^{pc-/-}$ cancer cells that might illuminate mechanisms involved in the recruitment of MDSCs by classifying the upregulated genes into either stroma- or tumor-enriched genes. To this end, the previously generated list of 242 genes with greater than 2-fold increased expression in *Pten*$^{pc-/-}$*Smad4*$^{pc-/-}$ relative to *Pten*$^{pc-/-}$ tumors[7] was intersected with 486 genes preferentially expressed in *Pten*$^{pc-/-}$*Smad4*$^{pc-/-}$ GFP+ cancer cells relative to Tomato+ stroma cells (fold change ≥4), yielding 28 genes that are markedly enriched in *Pten*$^{pc-/-}$*Smad4*$^{pc-/-}$ cancer cells. Among these 28 genes, *Cxcl5*, a key cytokine involved in MDSC recruitment[20,21], is the most significantly upregulated cancer cell-specific cytokine in *Pten*$^{pc-/-}$*Smad4*$^{pc-/-}$ tumors as compared to *Pten*$^{pc-/-}$ tumors (Figure 8B). Notably Cxcr2, the cognate receptor for Cxcl5, is also upregulated in *Pten*$^{pc-/-}$*Smad4*$^{pc-/-}$ tumors as compared to *Pten*$^{pc-/-}$ tumors and is significantly enriched in *Pten*$^{pc-/-}$*Smad4*$^{pc-/-}$ Tomato^{+} stroma cells (Figure 8B).

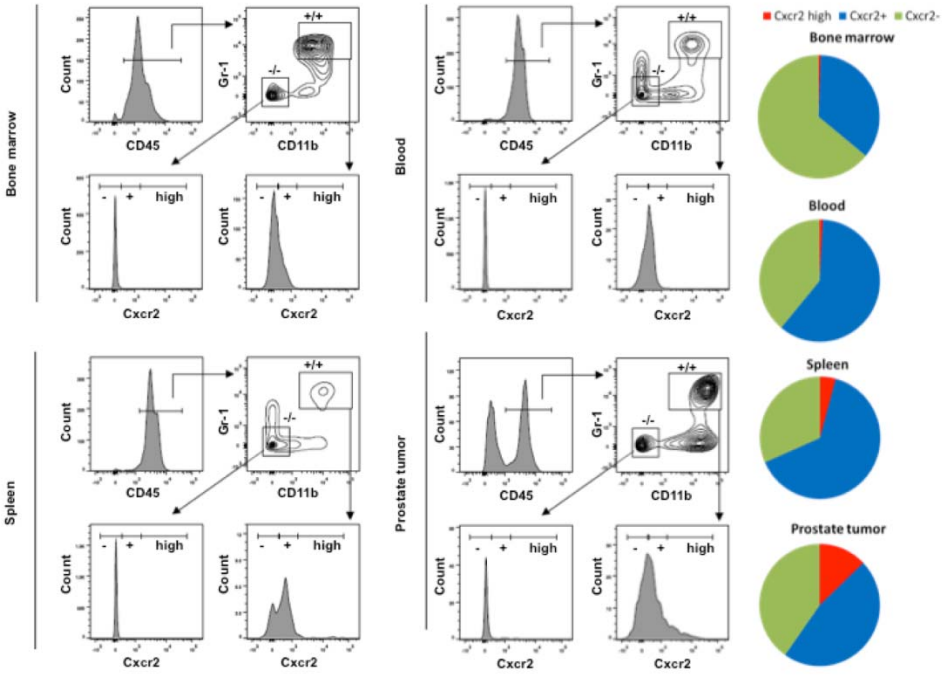

Figure 9. Prostate tumor enriches for CD11b+ Gr-1+ cells with higher Cxcr2 expression. From Pten/Smad4 mice with established prostate tumor, tissues including bone marrow, blood, spleen and prostate were harvested and stained with CD45, CD11b, Gr-1 and Cxcr2. From CD45+ cells in each tissue, both CD11b+ Gr-1+ cells and CD11b- Gr-1- cells were examined for Cxcr2 expression level. Cxcr2 expression is segmented to three levels: negative, positive and high, and CD11b+ Gr-1+ cells in each tissue are plotted for the three levels in pie charts (n=3).

The upregulation of Cxcl5 expression in *Pten*$^{pc-/-}$*Smad4*$^{pc-/-}$ prostate tumors was further confirmed by IHC (Figure 8C). In addition, I performed FACS analysis of CD11b^{+} Gr-1^{+} cells and CD11b^{-} Gr-1^{-} cells from bone marrow, spleen, peripheral blood, and tumors for Cxcr2 expression. As shown in Figure 9, CD11b^{-} Gr-1^{-} cells (largely lymphocytes) are devoid of Cxcr2 expression, whereas a large fraction of CD11b^{+} Gr-1^{+} cells express Cxcr2. When Cxcr2 expression was further separated into Cxcr2^{high} and Cxcr2^{+}, I observed an enrichment of the Cxcr2^{high} subpopulations in the CD11b^{+} Gr-1^{+} cells in prostate tumor compared with CD11b^{+} Gr-1^{+} cells from bone marrow, spleen or blood. This is consistent with the hypothesis of active recruitment of MDSCs by tumors through Cxcr2-mediated chemoattraction. So far, this part of study has started to address the task in Year 2 (**SOW Task 3**) and will be closely followed with *in vitro* and *in vivo* functional validation.

References

1 Karlou, M., Tzelepi, V. & Efstathiou, E. *Nat Rev Urol* **7**, 494-509 (2010).
2 Junttila, M. R. & de Sauvage, F. J. *Nature* **501**, 346-354 (2013).
3 Hanahan, D. & Coussens, L. *Cancer Cell* **21**, 309-322 (2012).
4 Talmadge, J. E. & Gabrilovich, D. I. *Nat Rev Cancer* **13**, 739-752 (2013).
5 Garcia, A. J. *et al. Molecular and cellular biology* **34**, 2017-2028 (2014).
6 Di Mitri, D. *et al. Nature* **515**, 134-137 (2014).
7 Ding, Z. *et al. Nature* **470**, 269-273 (2011).
8 Qin, H. *et al. Nat Med* **20**, 676-681 (2014).
9 Bjornson, Z. B., Nolan, G. P. & Fantl, W. J. *Current opinion in immunology* **25**, 484-494 (2013).
10 Youn, J. I., Nagaraj, S., Collazo, M. & Gabrilovich, D. I. *Journal of Immunology* **181**, 5791-5802 (2008).
11 Kusmartsev, S., Nefedova, Y., Yoder, D. & Gabrilovich, D. I. *J. Immunol.* **172**, 989-999 (2004).
12 Szuster-Ciesielska, A., Hryciuk-Umer, E., Stepulak, A., Kupisz, K. & Kandefer-Szerszen, M. *Acta Oncol.* **43**, 252-258 (2004).
13 Schmielau, J. & Finn, O. J. *Cancer Res.* **61**, 4756-4760 (2001).
14 Pekarek, L. A., Starr, B. A., Toledano, A. Y. & Schreiber, H. *The Journal of experimental medicine* **181**, 435-440 (1995).
15 Wang, G. *et al. Nat Genet* **45**, 739-746 (2013).
16 Lunardi, A. *et al. Nat Genet* **45**, 747-755 (2013).
17 Liu, F., Song, Y. & Liu, D. *Gene therapy* **6**, 1258-1266 (1999).
18 Ding, Z. *et al. Nature* **470**, 269-273 (2011).
19 Muzumdar, M. D., Tasic, B., Miyamichi, K., Li, L. & Luo, L. *Genesis* **45**, 593-605 (2007).
20 Yang, L. *et al. Cancer Cell* **13**, 23-35 (2008).
21 Bierie, B. *et al. Cancer Res* **68**, 1809-1819 (2008).

- **What opportunities for training and professional development has the project provided?**

Professional development: With the conducted research supported by the grant, the PI Xin Lu had the opportunity for the following conferences and workshops:
1) BD Biosciences course "Multicolor Flow Cytometry - Beyond the Basics". **Certificate awarded**. Sep 16-18, 2014. San Jose, CA
2) Society For Immunotherapy of Cancer (SITC) Annual Meeting. Nov 6-9, 2014, National Harbor, MD
3) 22nd Annual Prostate Cancer Foundation (PCF) Scientific Retreat. **Poster presentation**. Oct 8-10, 2015. Washington, DC

- **How were the results disseminated to communities of interest?**

The propose research, after presented and disseminated through conferences, has attracted interests from young professionals including two individuals who have participated in the study under the supervision of Xin Lu: **Sunada Khadka**, CPRIT-CURE Summer Intern at MD Anderson Cancer Center, college student at Wesleyan College, Macon, Georgia; **Jeong Woo Han**, high school sophomore, Michael E. DeBakey HSHP, Houston, Texas. Both students expressed strong interest in career on biomedical research after exposed in this research project.

- **What do you plan to do during the next reporting period to accomplish the goals?**

Next year's main goal will be to sample and profile MDSCs and associated cancer cells at different stages of the tumor development in order to build an signaling interactome between these two cell entities to explain how cancer cells signal to recruit and activate MDSCs, as well as how MDSCs directly or indirectly impact cancer cell proliferation and metastasis. My preliminary data suggest that Cxcl5-Cxcr2 signaling axis may mediate the recruitment of MDSCs. Therefore, this axis will be functionally validated both *in vitro* and *in vivo*. Specifically, the following aims will be achieved:

1) Deplete MDSCs with CD11b-DTR inducible allele in the mouse model and monitor effects on tumor growth and metastasis with bioluminescence imaging
2) Perform tumor-MDSC recombination experiment to evaluate the tumor-promoting function of MDSCs
3) Microarray profiling, RPPA and cytokine array of MDSCs and associated tumor cells
4) Integrated computational analysis of microarray and proteomic data
5) Tumor-to-MDSC and MDSC-to-tumor signaling validation with *in vitro and in vivo* assays, in particular, I will start to test if neutralizing Cxcl5-Cxcr2 signaling with antibodies or Cxcr2 inhibitor will abolish MDSC migration towards cancer cells in the *in vitro* migration assay. To test if targeting this signaling axis may reduce MDSC infiltration and have impact on tumor progression, Cxcr2 inhibitor SB255002 will be used to treat $Pten^{pc-/-}Smad4^{pc-/-}$ mice to examine if blocking the Cxcr2 signaling may elicit similar MDSC decrease and tumor inhibition as seen with Gr-1 antibody or anti-MDSC peptibody.

4. IMPACT

- **What was the impact on the development of the principal discipline(s) of the project?**

The first year research has built a solid foundation on the functional importance of the myeloid derived suppressor cells (MDSCs) in the progression of prostate cancer in the transgenic mouse model I use. It is clear that MDSCs accumulate inside the tumor and blood as the cancer progresses in the model, and MDSCs exert a potent immunosuppressive activity towards T cell proliferation. More importantly, ablation of the MDSCs using two independent biological agents significantly impedes the development of the cancer, in terms of both tumor size as well as histopathology. Due to the strong histology and molecular similarity of the model to the lethal form of human prostate cancer, my finding has profound implication on the prostate cancer basic research field as well as clinical care of prostate cancer. It is possible that targeting MDSCs represent a valid approach to effective control of aggressive prostate cancer in future.

- **What was the impact on other disciplines?**

The finding that MDSCs are potent immunosuppressors in the tumor microenvironment of prostate cancer has an overarching impact on the field of immunotherapy. Immunotherapy has been established as an additional pillar in the treatment of cancer, especially with recent development of immune checkpoint blockers like anti-PD1 and anti-CTLA4 antibodies. Nevertheless, the immunotherapy on prostate cancer and some other cancer types using such immune checkpoint blockade approach as monotherapy has been unsuccessful so far. My result suggests that combination targeting of both T cells and immunosuppressive cells such as MDSCs may hold the promise for synergistic efficacy to achieve better performance of cancer immunotherapy for prostate cancer and possibly other cancer types.

- **What was the impact on technology transfer?**

At the completion of first year of proposed research, there is nothing to report on this aspect yet.

- **What was the impact on society beyond science and technology?**

At the completion of first year of proposed research, there is nothing to report on this aspect yet.

5. CHANGES/PROBLEMS

Nothing to report.

6. PRODUCTS

Nothing to report.

7. PARTICIPANTS & OTHER COLLABORATING ORGANIZATIONS

- **What individuals have worked on the project?**

Name:	*Xin Lu*
Project Role:	*Instructor*
Researcher Identifier (e.g. ORCID ID):	*189447 (MD Anderson Cancer Center Employee ID)*
Nearest person month worked:	*12*
Contribution to Project:	*No change*
Funding Support:	*No change*

Name:	*Guocan Wang*
Project Role:	*Postdoc Fellow*
Researcher Identifier (e.g. ORCID ID):	*Not applicable*
Nearest person month worked:	*3*
Contribution to Project:	*Dr. Wang has performed the work in the depletion experiment including drug treatment and histology analyses.*
Funding Support:	Prostate Cancer Research Program (PCRP) W81XWH-13-1-0202

Name:	*Prasenjit Dey*
Project Role:	*Postdoc Fellow*
Researcher Identifier (e.g. ORCID ID):	*Not applicable*
Nearest person month worked:	*1*
Contribution to Project:	*Dr. Dey has performed the work in the immunosuppression assay*
Funding Support:	Prostate Cancer Research Program (PCRP) W81XWH-14-1-0429

- **Has there been a change in the active other support of the PD/PI(s) or senior/key personnel since the last reporting period?**

Nothing to report.

- **What other organizations were involved as partners?**

Nothing to report.

8. SPECIAL REPORTING REQUIREMENTS

Nothing to report.

9. APPENDICES:

Nothing to report.